Ancient TL

www.ancienttl.org · ISSN: 2693-0935

Rosenzweig, R. and Porat, N., 2015. *Evaluation of soil-moisture content for OSL dating using an infiltration model.* Ancient TL 33(2): 10-14. https://doi.org/10.26034/la.atl.2015.494

Ancient TL

Evaluation of soil-moisture content for OSL dating using an infiltration model

Ravid Rosenzweig[1]* and Naomi Porat[1]

[1]Geological Survey of Israel, 30 Malkhei Israel St., Jerusalem 95501, Israel

*Corresponding Author: rravid@gsi.gov

Received: September 12, 2015; in final form: December 3, 2015

Abstract

Uncertainty in soil-moisture content estimation can introduce large errors into calculation of OSL ages. In the current paper we evaluate the soil-moisture content by using an infiltration model which encompasses site-specific information regarding the climatic conditions and soil properties. The model provides the variation of the soil-moisture content with depth and time. It also provides clear uncertainty bounds for the estimated soil-moisture profile which serves as a measure for model reliability. The current approach is implemented to calculate the soil-moisture profile of a Late-Holocene, open-structure soil section subjected to Mediterranean climate in which hot and dry summers and cool and wet winters generate large variation in the moisture-content. We show that the model can improve soil-moisture estimation, reducing the associated uncertainty and accounting for the depth from the soil surface. These estimates can then be used to better constrain uncertainties in OSL dose rate calculations.

Keywords: moisture content

1. Introduction

The importance of estimating time-averaged moisture contents for accurate OSL dating cannot be underestimated. Large uncertainties in moisture contents introduce large errors into the ages. For example, assumption of a moisture fraction of 20% instead of 10% g/g of sample, will decrease dose rate to 'coarse grains' and increase the calculated age by ∼10% (Aitken, 1985, p. 76).

Mediterranean climate typically has large differences between summer and winter, with hot and dry summers and cool and moist winters, resulting in great variability in soil moisture. A single sample cannot capture the average annual moisture contents due to these large variations in precipitation and evaporation, particularly as the beginning and end of the rainy season vary greatly from year to year.

While our ability to reconstruct soil moisture contents for past climates is limited, we can in the least get a good handle on current seasonal variations. Lowick & Preusser (2009) have reconstructed the soil-moisture of saturated samples that have desiccated, but no attempt was made to assess the mean moisture content in the unsaturated zone. Recently, Nelson & Rittenour (2015) used grain-size distribution and maps of the annual mean water state (mean matric head) to calculate the mean moisture content of Holocene sediments from Kebab Creek, Utah for OSL dating.

While the work of Nelson & Rittenour (2015) provides a simple way to calculate soil moisture content based on large-scale soil properties maps, we take a different approach and obtain soil moisture content by using an infiltration model which incorporates site-specific climatic data combined with grain size and density measurements. The addition of bulk density measurements to the grain size data improves by a great deal the assessment of the water content (Schaap et al., 2001). We also give uncertainty bounds to the calculation, providing a confidence interval for the soil-moisture. The model provides the full variability of soil moisture in time and space, thus allowing to specifically consider the effect of depth on the moisture content. We demonstrate the use of the procedure by applying it to predict the moisture content of anthropogenic soil within archaeological farming terraces of Late Holocene age, with open-structure soil prone to evaporation (Gadot et al., 2015). The results are then used in the age calculations to assess the impact of the moisture content on the ages.

	Jan	Feb	Mar	Apr	May	June	July	Aug	Sep	Oct	Nov	Dec
Rainfall (mm)	133.2	118.3	92.7	24.5	3.2					15.4	60.8	105.7
Rainy days	9.7	8.7	7.6	2.7	0.7					1.9	5.5	7.9
Daily evaporation (mm)	2.5	2.8	4.2	5.7	6.5	6.9	7.1	6.5	5.6	5	4	2.8

Table 1. Climatic conditions near Har-Eitan (evaporation and rain data averaged for 1988-2000 and 1970-2000, respectively)

2. Research site

The area is the limestone highlands of central Israel located within the Mediterranean climate zone. The study was conducted at Har (Mount) Eitan, a hilly spur almost 800 m high about 10 km west of Jerusalem. In this area, the limestone slopes are covered with archaeological bench terraces, created from stone walls back-filled with soil. Pits were excavated for OSL dating within the framework of a larger study on the terracing of the Judea Mountains (Gadot et al., 2015). For accurate dating of terrace construction, we needed to know the average annual moisture content for samples located at depths from 0.25 to 2.0 m.

The climatic data used in the model were taken from the database of the Israeli Meteorological Service (http://www.ims.gov.il). Precipitation data were taken from a meteorological station in Jerusalem located 10.5 km east of Har-Eitan while evaporation data was taken from Rosh-Zurim meteorological station located 11 km south east to Har-Eitan; both stations are the closest to the study area. The monthly-averaged climatic conditions for Har-Eitan are given in Table 1. The rainy period lasts from November to April with an average of 45 rainy days and an average annual rainfall of 554 mm. Mean daily class A pan evaporation (potential evaporation; Jarraud, 2008) varies from 7.1 mm in July to 2.5 mm in January.

3. Methods

Twenty four samples taken at different depths along the open excavated pits (Fig. 1) were analyzed for particle size distribution (PSD; smaller than 2 mm). The average soil PSD for the sand, silt and clay fractions and their respective standard deviation, and the PSD of two additional samples that were used to evaluate the sensitivity of the model to soil texture, are presented in Table 2.

	% Sand	% Silt	% Clay
Average	38.3 (11.4)	55 (11)	6.7 (1.9)
Highest silt	11.4	80.4	8.2
Lowest silt	58.4	35.7	5.9

Table 2. Particle size distribution (< 2 mm) for soil samples from Har-Eitan terraces. Values in parentheses represent standard deviation.

Gravimetric water content (or mass fraction moisture) was measured in winter (about a week after a rain event) and in the summer by the gravimetric method (Dane & Topp, 2002) on samples taken at different depths in the pits.

Figure 1. A typical soil profile of one of the pits in Har-Eitan. The holes in the profile represent the locations where undisturbed soil or other samples were taken. Insert: The sampling ring and ring holder used to take the undisturbed samples.

The average gravimetric water content in the summer was 5.5% $\pm$ 1.2% g/g (N=5) whereas the average gravimetric water content after rain was 24% $\pm$ 2% g/g (N=6; Table 3). Bulk density was measured on undisturbed soil samples of known volume. The average bulk density for this particular area was found to be $1.10 \pm 0.12\ g/cm^3$ (N=5). Bulk density is important since it is directly related to cosmic radiation attenuation (Prescott & Hutton, 1994) and indirectly to both beta and gamma dose rates through soil moisture content.

Pit	Depth (cm)	Gravimetric water content (g/g)
A4	60	0.20
A4	33	0.26
A4	27	0.27
A1	75	0.24
A1	22	0.23
A1	50	0.23
Average	44.5 (20.7)	0.24 (0.02)

Table 3. Measurements of gravimetric water content at Har-Eitan. Samples were taken during the winter of 2014-15, approximately one week after a rain event. Values in parentheses represent standard deviations.

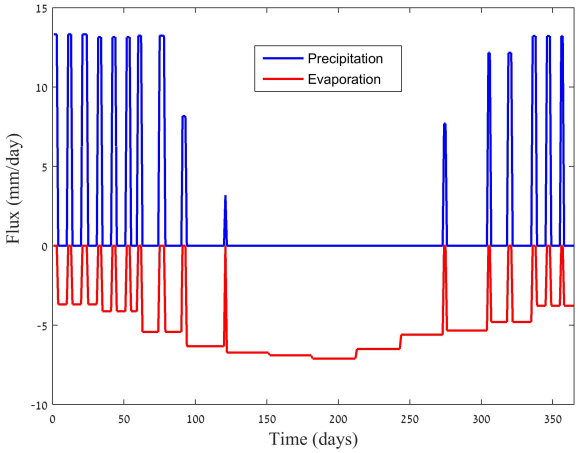

Figure 2. Precipitation and evaporation fluxes specified for the model over a year. Evaporation is defined as a negative flux.

4. Model Setup

In this work we use a one dimensional (1D) infiltration model to evaluate the mean annual water content in the soil. The model allows calculation of variation in water content with depth by solving the soil-water dynamics while incorporating data of the soil PSD and climatic conditions. The model provides the water content profile with much higher certainty than the one obtained from one or two measurement at random points in time, as it provides the full temporal and spatial variations.

We use Hydrus 1D (http://www.pc-progress.com/en/Default.aspx?hydrus-1d), a free code developed by the US salinity lab to model water flow and water content within the soil (Šimůnek et al., 2008). Hydrus 1D describes variably-saturated water flow by solving the Richard's equation

$$\frac{\partial\theta}{\partial t} = \frac{\partial}{\partial z}\cdot\left(K(h)\frac{\partial h}{\partial z}\right) + \frac{\partial K}{\partial z} \tag{1}$$

where θ is the volumetric water content, h the matric head, t the time, z the vertical coordinate and $K(h)$ the unsaturated hydraulic conductivity which is a function of the matric head. We note that the volumetric water content (volume of water per total volume of soil in units of cm^3/cm^3) commonly used in infiltration models is a different measure of soil moisture than the gravimetric water content (water weight per dry soil weight in units of g/g) used in dose rate calculations for luminescence dating. The conversion from gravimetric to volumetric water content is given by $\theta = \omega\cdot\rho_b/\rho_w$ where ω is the gravimetric water content, ρ_b is the bulk soil density and ρ_w is the density of water, commonly taken as 1 g/cm^3 .

To solve Equation 1, relations for the hydraulic conductivity function and for the soil water-retention curve $(\theta(h))$ are needed. We use the van Genuchten and van Genuchten-Mualem models (Mualem, 1976; van Genuchten, 1980) for the soil water retention curve

$$Se = [1+(\alpha\mid h_m\mid)^n]^{-m} \tag{2}$$

and hydraulic conductivity, respectively,

$$K = K_S\sqrt{Se}\left[1-\left(1-Se^{1/m}\right)^m\right]^2 \tag{3}$$

where α, n and $m = 1-1/n$ are empiric parameters which depend on the soil pore size distribution, K_S is the saturated hydraulic conductivity and $Se = (\theta-\theta_r)/(\theta_s-\theta_r)$ is the effective saturation where θ_s is the porosity and θ_r is the irreducible water content. The porosity and irreducible water content represent the upper and lower bounds of the water content in soil, respectively.

The modeled domain represents a profile of 10 m depth of homogeneous soil. Although Har-Eitan consists of bedrock at 2 m depth at most, it was decided to ignore it since it is highly fractured and the fractures are filled with the natural soil. Thus, the bedrock is not expected to impede water flow downwards. Boundary conditions for the model were assigned as atmospheric boundary condition at the soil surface and free-drainage condition (i.e., $\frac{\partial\theta}{\partial z}=0$) at the lower boundary. The atmospheric boundary condition represents either an evaporation flux out of the soil surface or a precipitation flux into the soil surface. Daily fluxes were calculated from the daily average of potential evaporation, the monthly average of precipitation and the average number of rainy days for each month (Table 1). It was assumed that each rain event lasts for 3 days and that on rainy days the potential evaporation is zero. The daily evaporation and precipitation fluxes put into the model are shown in Figure 2.

The value of the soil hydraulic parameters (α, n, m and K_S) presents the greatest uncertainty in unsaturated flow models. In the current work, the hydraulic parameters of the soil were determined as follows (Table 4): the porosity θ_s and irreducible water content θ_r were assigned as constants. The porosity was calculated using the relation $\theta_s = 1-\rho_b/\rho_s$ where ρ_s is the grain density. Porosity was calculated based on the measured bulk density and by assuming a grain density of 2.65 g/cm^3 .

The irreducible water content was assigned as the minimal value in the range of water content measured in summer at the surface of the open holes (5%). Summer water content was also used as the minimum water content by Burbidge et al. (2014). The other parameters α, n, and K_S were predicted by ROSETTA (http://www.ars.usda.gov/News/docs.htm?docid=8953), a free computer program developed by the US salinity lab that predicts the soil hydraulic properties using a neural network analysis based on the soil grain size distribution and bulk density (Schaap et al., 2001). The program uses a large dataset which contains properties of more than 2000 soils. It provides average values and uncertainty bounds for each parameter.

The soil profile was discretized into 201 nodes where the grid was refined near the soil surface and spacing was gradually increased towards the deeper sections of the profile. The model was left to run for 300 years to achieve a temporally

Soil structure	θ_r cm^3/cm^3	θ_s cm^3/cm^3	$\alpha(1/m)$			n			K_S m/day		
			Average	High	Low	Average	High	Low	Average	High	Low
Average	0.055	0.58	0.51	0.637	0.4063	1.6608	1.736	1.588	1.422	2.095	0.9654
Highest-silt			0.43	0.631	0.293	1.745	1.878	1.621	1.2167	2.386	0.621
Lowest-silt			1.58	1.88	1.33	1.452	1.518	1.393	1.7084	2.44	1.1962

Table 4. Soil hydraulic properties used in the model for the three soil structures. Average, high and low values of α, n and K_S represent the average, the high and the low bounds predicted by ROSETTA.

periodic condition where no change in the results was observed from one year to the next.

To evaluate the sensitivity of the mean annual water content to the hydraulic parameters and soil composition, hydraulic parameters were predicted for 3 PSD's (Table 2). The first was obtained by averaging all 24 soil samples taken from the terraces, the other two represent individual samples having the highest and lowest silt fraction and the lowest and highest sand fraction, respectively (Highest silt and Lowest silt in Table 2). Hydraulic parameters were predicted for each soil structure (Table 4) and models were run for sets of hydraulic parameters which represent combinations of the average/ lowest/ highest or intermediate values predicted for the different parameters. The water content measured on samples taken during winter was considered as the maximal water content (Burbidge et al., 2014) and was used to calibrate the models such that only runs that yielded a winter (after rainfall) water content of 26% $\pm$ 2% cm^3/cm^3 at a depth of 50 cm were included in the analysis. This range corresponds to the average volumetric water content $\pm$ one standard deviation measured at an average depth of $\sim$50 cm (Table 3). We note that since measurements of winter water content were taken once in 2015 while the model is based on multi-year average climatic data, some flexibility in the maximal water content is allowed by specifying this range.

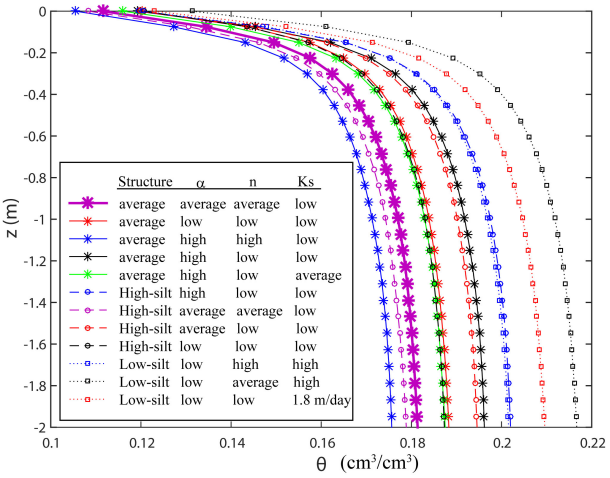

Figure 3. Average annual water content profile obtained for the three soil compositions and for different sets of soil hydraulic properties. Asterisks and solid lines - average soil; circles and dashed lines - highest-silt soil; squares and dotted lines - lowest silt water soil. The purple, solid, thick curve represents the water content profile which was obtained for the predicted average α and n values for the average soil composition.

5. Results and Discussion

The profile of the average annual water content is displayed in Figure 3. The water content profile was obtained for the three investigated soil compositions and for combination of different sets of soil-hydraulic properties that lie within the uncertainty bounds for each soil type. It is shown that near the soil surface the water content and its variability ($\pm$ 1.5%) are lower than in the deeper sections of the profile since the water content is influenced by water evaporation from the soil. At larger depths, there is a greater variability in water content (approx. $\pm$ 2%, at 2 m) that depends on soil composition and soil-hydraulic properties. It is shown that for each curve, the annual average water content for a given soil composition, under present conditions, is approximately constant at depths greater than 0.6 m. This is because deeper in the section evaporation no longer affects soil moisture. This "constant moisture" depth is expected to change with the soil type and the value of potential evaporation.

For the average soil composition, the water content measured after rain limited the saturated hydraulic conductivity to the low-to-average values of the predicted range. The water content obtained for the average α and n values and low K_S (the thick purple curve on Fig. 3) is 0.170 cm^3/cm^3 and 0.177 cm^3/cm^3at depth of 0.5 and 1 m, respectively. Considering all the curves obtained for the average soil composition, the annual average water content can be estimated as 0.174 $\pm$ 0.01 cm^3/cm^3 and 0.182 $\pm$ 0.01 cm^3/cm^3 at depth of 0.5 and 1 m, respectively. This corresponds to gravimetric water content (as used in dose rate calculations for luminescence dating) of 0.158 $\pm$ 0.009 g/g and 0.165 $\pm$ 0.009 g/g at depth of 0.5 and 1 m, respectively.

Naturally, when taking into account the Highest-silt and Lowest-silt soil compositions, the uncertainty in predicting the water content increases. Figure 3 shows that the Lowest-silt soil yields higher water content. This is the result of the larger α values predicted for this soil structure. Generally speaking, larger values result in a lower infiltration rate which leaves the soil wetter. Still, the range of the water content remains rather small with the volumetric water content estimated as 0.180 $\pm$ 0.016 cm^3/cm^3 and 0.192 $\pm$ 0.02 cm^3/cm^3 at depth of 0.5 and 1 m, respectively. The corresponding gravimetric water contents are 0.163 $\pm$ 0.0145 g/g and 0.174 $\pm$ 0.018 g/g. These estimated values have much lower uncertainty bounds than the uncertainties com-

monly used in OSL dating.

Using this range of values to calculate dose rates and ages for a typical sample from Har-Eitan at a depth of 0.5 m, we obtain an age range of 1780-1800 or 1770-1800 years for the better or less constrained soil composition, respectively, well within any error range of an OSL age.

Naturally, this model has several limitations. First, as most conventional models of flow in unsaturated conditions, it does not directly consider effects such as water repellency and swelling. To account for these, one would have to measure the soil water retention curve to directly calibrate the soil hydraulic properties. In most studies, however, these effects are traditionally ignored.

Second, the model is based on modern climatic conditions. Long-term changes in rainfall, temperature and vegetation (affecting evapotranspiration) will obviously affect soil moisture content. However, given the limited data on past conditions and its low resolution, our starting point is modern climatic conditions. Using paleoclimate data, one could extrapolate the results to past conditions; however this is beyond the scope of the current paper.

6. Conclusions

Average annual soil moisture profiles were calculated using an infiltration model encompassing climatic data and soil properties. This estimation has several advantages over the conventional way water content is estimated for OSL dating and over recent contributions in the field. First, it is physically based and encompasses data of the site-specific climatic conditions and soil structure. Second, it accounts for variation of the water content with the soil depth; and last, it provides clear uncertainty bounds and reduces the variability in the water content estimation and thus in the luminescence age. Furthermore, bulk density (or at least porosity) measurements can also improve estimates of the cosmic dose rate contribution to the dose rate.

To predict moisture contents, monthly average data of rainfall and evaporation are needed together with soil grain size distribution, bulk density and water content measurement in winter and summer. If no bulk density and summer water content measurements are available, one can predict the soil hydraulic properties based on the grain size distribution alone (using ROSETTA). This is, however, not recommended as the associated uncertainty of this prediction is much larger.

The model shows two regions within the soil profile; the upper part in which moisture content is more dependent on evaporation and less on soil type, and the lower part in which moisture content is mostly a function of soil properties and is relatively constant with depth. In our study area, the transition between these two regions occurs roughly at 0.6 m. This depth, however, is expected to be site-specific and related to the soil type and evaporation rate.

Acknowledgments

The research was supported by an Israel Science Foundation grant (Grant 0606714492) awarded to Naomi Porat and Yuval Gadot.

References

Aitken, M.J. *Thermoluminescence dating*. Studies in archaeological science. Academic Press, 1985.

Burbidge, C., Trindade, M., Dias, M., Oosterbeek, L., Scarre, C., Rosina, P., Cruz, A., Cura, S., Cura, P., and Caron, L. *Luminescence dating and associated analyses in transition landscapes of the alto ribatejo, Central Portugal*. Quaternary Geochronology, 20: 65–77, 2014.

Dane, J.H. and Topp, C.G. *Methods of soil analysis, part 4- physical methods. p. 1692*. Soil Science Society of America, Madison, 2002.

Gadot, Y., Davidovich, U., Avni, G., Avni, Y., and Porat, N. *The formation of terraced landscapes in the Judean Highlands, Israel*. Antiquity, 346, 2015. URL http://antiquity.ac.uk/projgall/gadot346. Project Gallery article.

Jarraud, M. *Guide to meteorological instruments and methods of observation (wmo-no. 8)*. World Meteorological Organisation: Geneva, Switzerland, 2008.

Lowick, S. and Preusser, F. *A method for retrospectively calculating the water content for silt-dominated desiccated core samples*. Ancient TL, 27: 1–5, 2009.

Mualem, Y. *New model for predicting hydraulic conductivity of unsaturated porous-media.* Water Resources Research, 12: 513–522, 1976.

Nelson, M.S. and Rittenour, T.M. *Using grain-size characteristics to model soil water content: Application to dose-rate calculation for luminescence dating.* Radiation Measurements, 81: 142–149, 2015.

Prescott, J.R. and Hutton, J.T. *Cosmic ray contributions to dose rates for luminescence and esr dating: Large depths and long-term time variations*. Radiation Measurements, 23: 497–500, 1994.

Schaap, M.G., Leij, F.J., and van Genuchten, M.Th. *Rosetta: A computer program for estimating soil hydraulic parameters with hierarchical pedotransfer functions*. Journal of Hydrology, 251: 163–176, 2001.

Šimůnek, J., van Genuchten, M.T., and Šejna, M. *Development and applications of the hydrus and stanmod software packages and related codes*. Vadose Zone Journal, 7: 587–600, 2008.

van Genuchten, M.T. *A closed-form equation for predicting the hydraulic conductivity of unsaturated soils*. Soil Science Society of America Journal, 44: 892–898, 1980.

Reviewer

Chris Burbidge